Supplemental Materials: Comparative Analysis of Nonlinear Viscoelastic Models Across Common Biomechanical Experiments

Will Zhang*,[1] Adela Capilnasiu*,[2] and David Nordsletten[3]

[1]*Department of Biomedical Engineering, University of Michigan, Ann Arbor, USA*
Tel.: 734-764-9588
[2]*School of Biomedical Engineering and Imaging Sciences, King's College London, London, UK*
Tel.: +44 (0)20 7836 5454
[3]*Department of Biomedical Engineering, University of Michigan, Ann Arbor, USA*
School of Biomedical Engineering and Imaging Sciences, King's College London, London, UK
Tel.: 734-764-9588

(Dated: January 22, 2021)

I. ADDITIONAL COMPARATIVE RESULTS ACROSS EXPERIMENTAL TEST CASES

As indicated in the main text, this paper considers 4,216 models across 144 test case scenarios. While specific results were presented in the paper as exemplars of the broader dataset, this supplement provides more data on the considered test cases. Specifically, we present further data comparing biaxial, pure shear, simple shear, torsion, relaxation and creep, illustrating the data shown in Fig. 5 and Fig. 6. Specifically, we present similarity scores for 0.05Hz and 5Hz, example curves in this range, and an analysis of the impact of stretch / shear.

II. BIAXIAL TEST CASE

For the biaxial kinematics, the parameters used are the same as that of the uniaxial test, reproduced for frequencies of 0.05 Hz and 5 Hz. Similarity scores are shown in Fig. S1, with the last cycle (of 5) shown in Fig. S2. The impact of loading and nonlinear parameters is highlighted in Fig. S3.

III. PURE SHEAR TEST CASE

The pure shear testing result are produced for sinusoidal loading with frequencies of 0.05 Hz and 5 Hz. Similarity scores are shown in Fig. S4, with the last cycle (of 5) shown in Fig. S5. The impact of loading and nonlinear parameters is highlighted in Fig. S6.

IV. SIMPLE SHEAR TEST CASE

The simple shear testing result are produced for sinusoidal loading with frequencies of 0.05 Hz and 5 Hz. Similarity scores are shown in Fig. S7, with the last cycle (of 5) shown in Fig. S8. The impact of loading and nonlinear parameters is highlighted in Fig. S9.

V. TORSION TEST CASE

The torsion testing result are produced for sinusoidal loading with frequencies of 0.05 Hz and 5 Hz. Similarity scores are shown in Fig. S10, with the last cycle (of 5) shown in Fig. S11. The impact of loading and nonlinear parameters is highlighted in Fig. S12.

---

*Authors acknowledge equal contributions toward first authorship

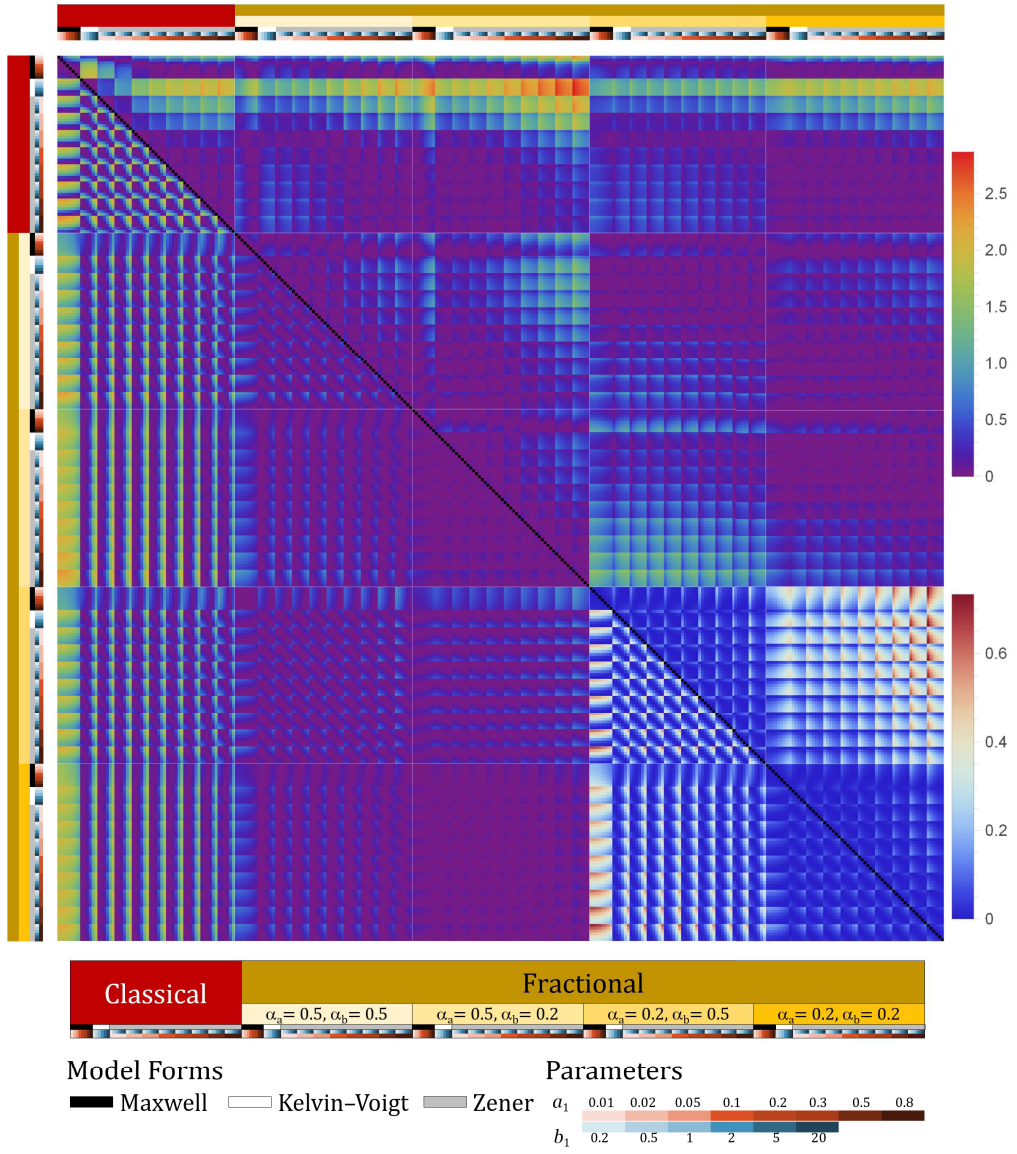

FIG. S1: An illustration using cyclic biaxial extension with a sine wave form as the example to show how the model responses compare to each other. Each cell shows the similarity score (Eq. 30) between two model forms. The bottom half of the array plot shows the comparison with a frequency of loading of 0.05 Hz and the top half at 5 Hz. The plots for $\alpha_a = 0.2$ uses a different color scale to show more details.

All cyclic investigations at 0.05 and 5 Hz offer the same insights as the uniaxial case presented in the main body of the study (Fig. 5). The classical Maxwell model is unsuitable for cyclic tests at low frequencies (0.05 Hz), but this trend changes as the frequency increases, with the classical Kelvin-Voigt model becoming more dissimilar compared to other model forms at 5 Hz. Moreover, the similarity pattern across $(\alpha_a, \alpha_b, a_1, b_1)$ parameter combinations (Figs. S2, S5, S8, S11) is the same as in Fig. 6, which indicates that for an isotropic material, the information extracted from multi-axial testing protocols is the same as for uniaxial testing. This is particularly applicable for smaller deformation levels (i.e. $\lambda = 1.1$ or $\gamma = 0.1$), as similarity patterns remain the same across tests (Figs. S3, S6, S9, S12 compared to Fig. 8). At higher deformation levels (i.e. i.e. $\lambda = 1.4$ or $\gamma = 0.4$), similarity across varying parameters changes, particularly in the biaxial case. This is triggered by the exacerbated nonlinearity in the biaxial test, as this test was pushed beyond typical deformation limits. This also indicates that tests probe the nonlinear material behavior at different deformation levels, with the biaxial test showing the most pronounced nonlinearity, followed, in order, by

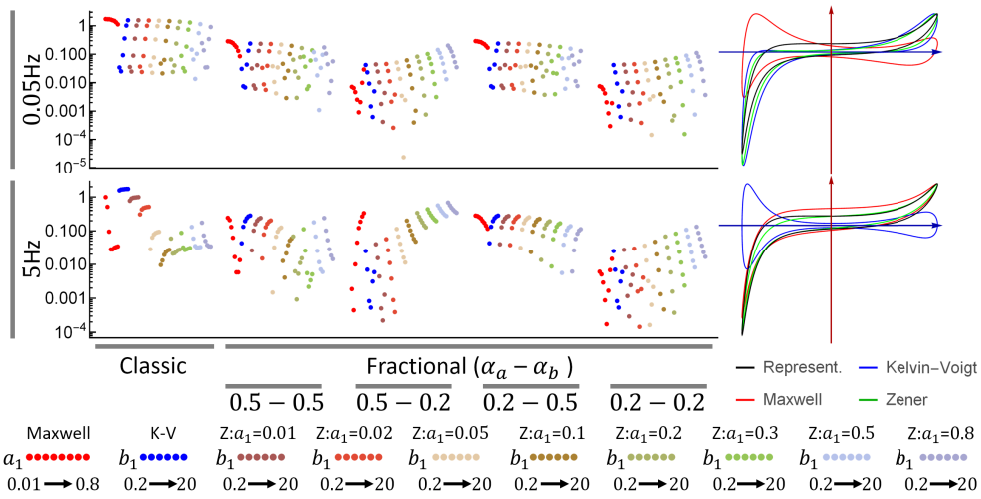

FIG. S2: Examination of each model form in comparison to a representative fractional Zener model exhibiting similar behavior to experimental data. Results at (top) 0.05 and (bottom) 5 Hz are shown. Scatter plots show the similarity scores (Eq. 30) for each model form and parameter combination on the left and the behavior of the *best case* (lowest similarity score) classical Maxwell, Kelvin-Voigt and Zener models on the right.

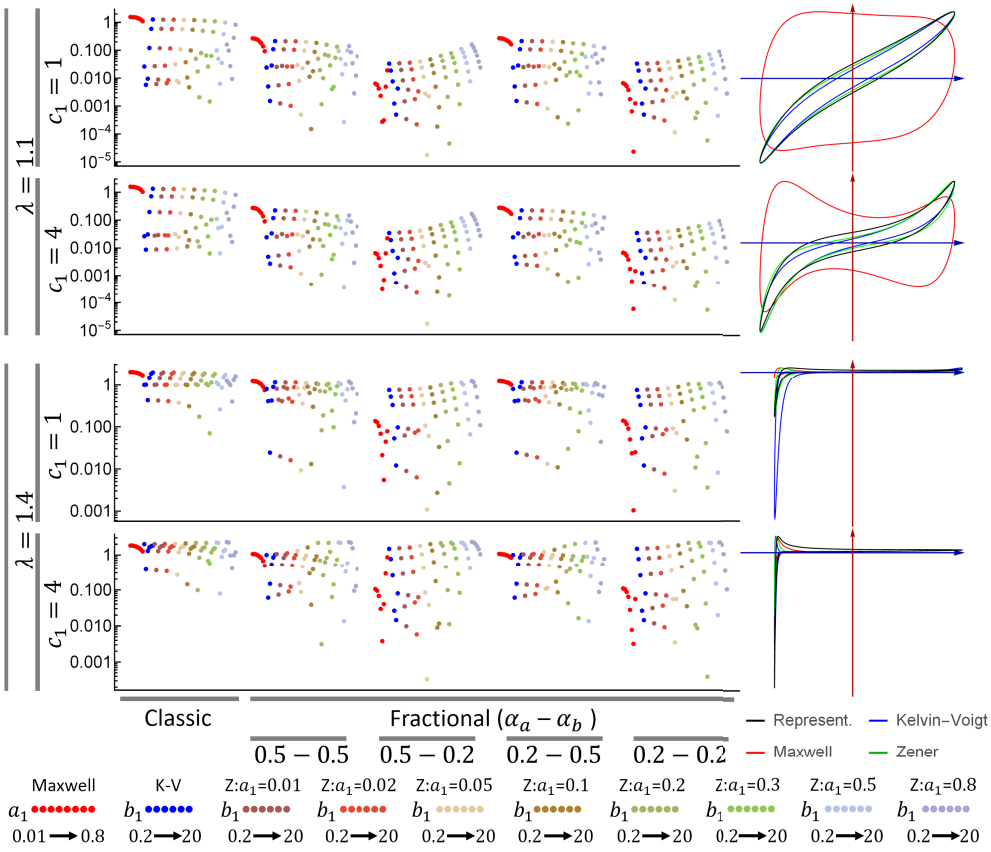

FIG. S3: Results shown the similarity scores at the maximum stretch of 1.1 and 1.4 (row 1&2 and 3&4, respectively) and two different nonlinearity parameters $c_1 = 1$ and $c_1 = 4$ (row 1&3 and 2&4, respectively).

pure shear, uniaxial, simple shear and torsional shear. Therefore, although the same characteristics can be extracted from isotropic tissues across all cyclic testing protocols, the nonlinearity may be better emphasized

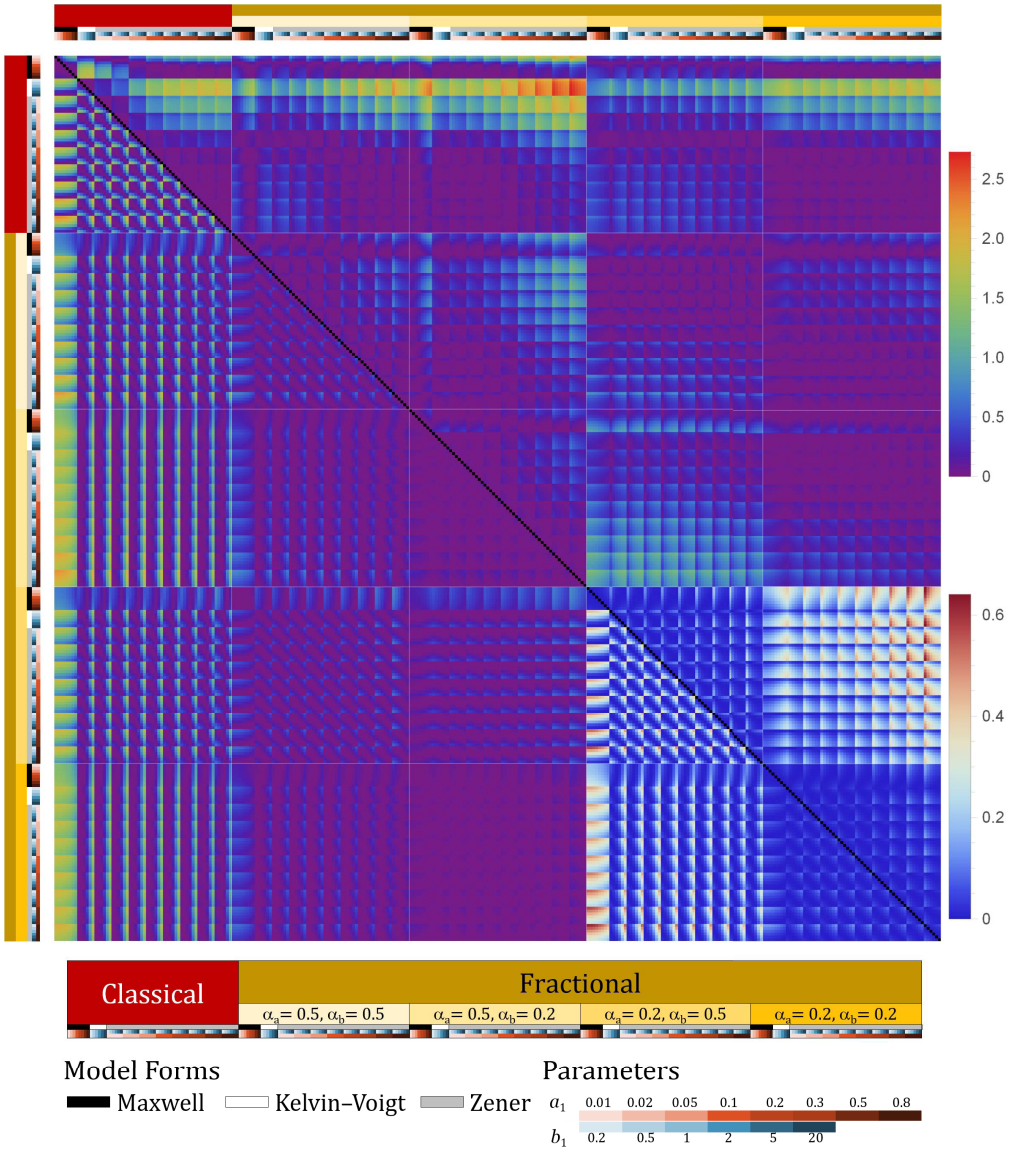

FIG. S4: An illustration using cyclic pure shear deformation with a sine wave form as the example to show how the model responses compare to each other. Each cell shows the similarity score (Eq. 30) between two model forms. The bottom half of the array plot shows the comparison with a frequency of loading of 0.05 Hz and the top half at 5 Hz. The plots for $\alpha_a = 0.2$ uses a different color scale to show more details.

through certain tests (e.g. uniaxial rather than simple shear).

VI. RELAXATION TEST CASE

The relaxation testing result are produced for durations of 0.5 seconds and 50 seconds. Each cycle consists of a loading phase and an unloading phase using that a_{step} function. The cycle is repeated three time with the last cycle shown below. Similarity scores are shown in Fig. S13, with the last cycle (of 3) shown in Fig. S14. The impact of loading and nonlinear parameters is highlighted in Fig. S15.

The test duration investigation of the relaxation protocol (Fig. S13) is comparable to the frequency investigation of oscillatory tests, as the classical Maxwell model is the most dissimilar at long test durations (50 s) and the classical Kelvin-Voigt or Zener model with low a_1 are more dissimilar with the rest of the

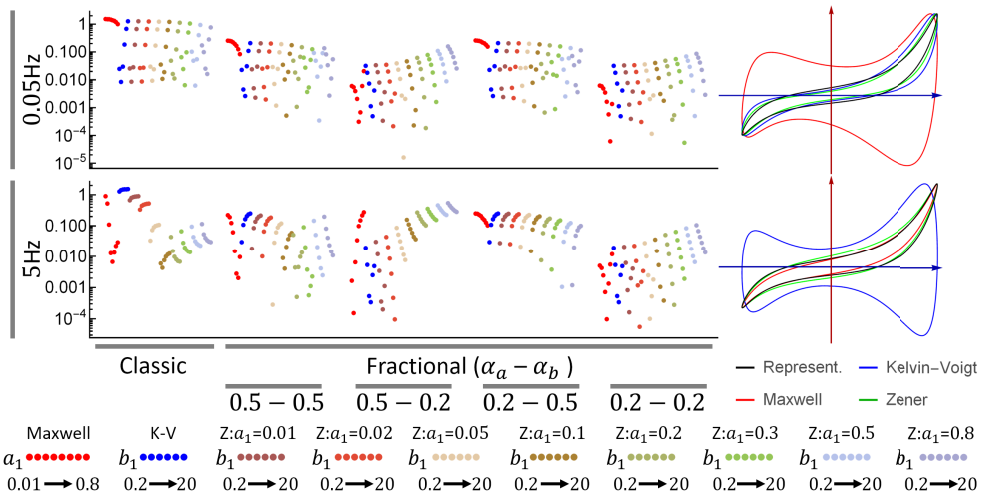

FIG. S5: Examination of each model form in comparison to a representative fractional Zener model exhibiting similar behavior to experimental data. Results at (top) 0.05 and (bottom) 5 Hz are shown. Scatter plots show the similarity scores (Eq. 30) for each model form and parameter combination on the left and the behavior of the *best case* (lowest similarity score) classical Maxwell, Kelvin-Voigt and Zener models on the right.

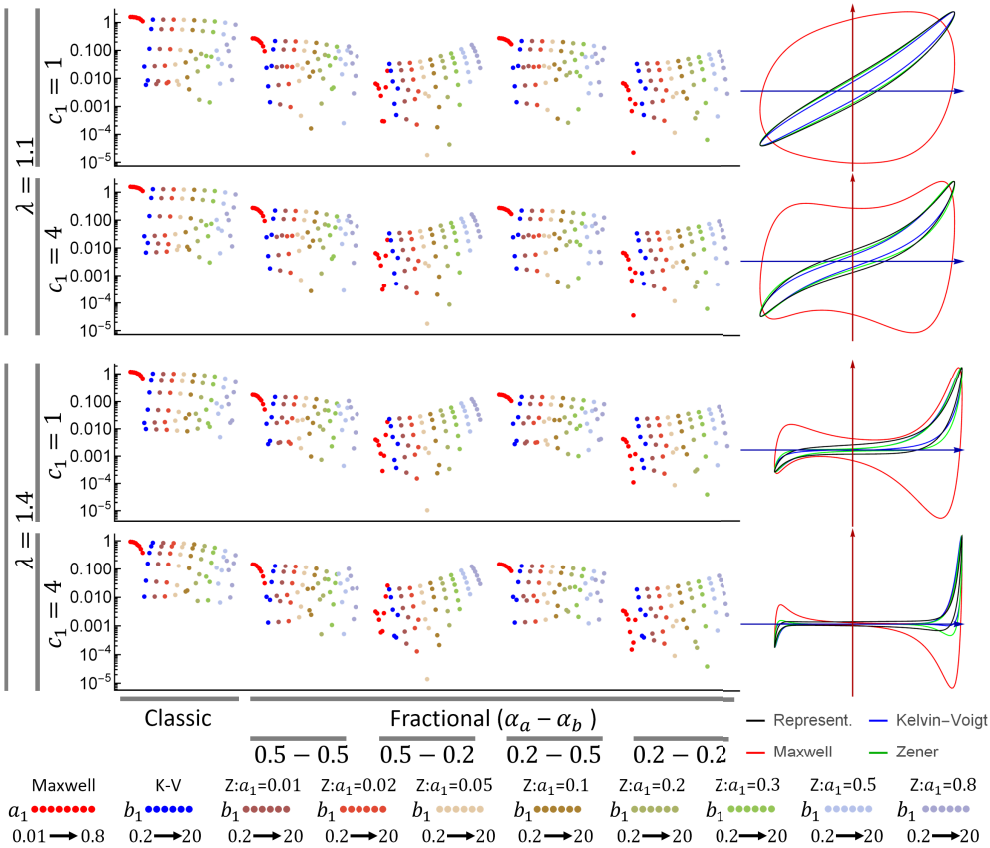

FIG. S6: Results shown the similarity scores at the maximum stretch of 1.1 and 1.4 (row 1&2 and 3&4, respectively) and two different nonlinearity parameters $c_1 = 1$ and $c_1 = 4$ (row 1&3 and 2&4, respectively).

tests at short test durations (0.5 s). At short test duration, the behavior of the fractional Zener model is comparable to the one at high duration, whereas the classical models show a different pattern than usually

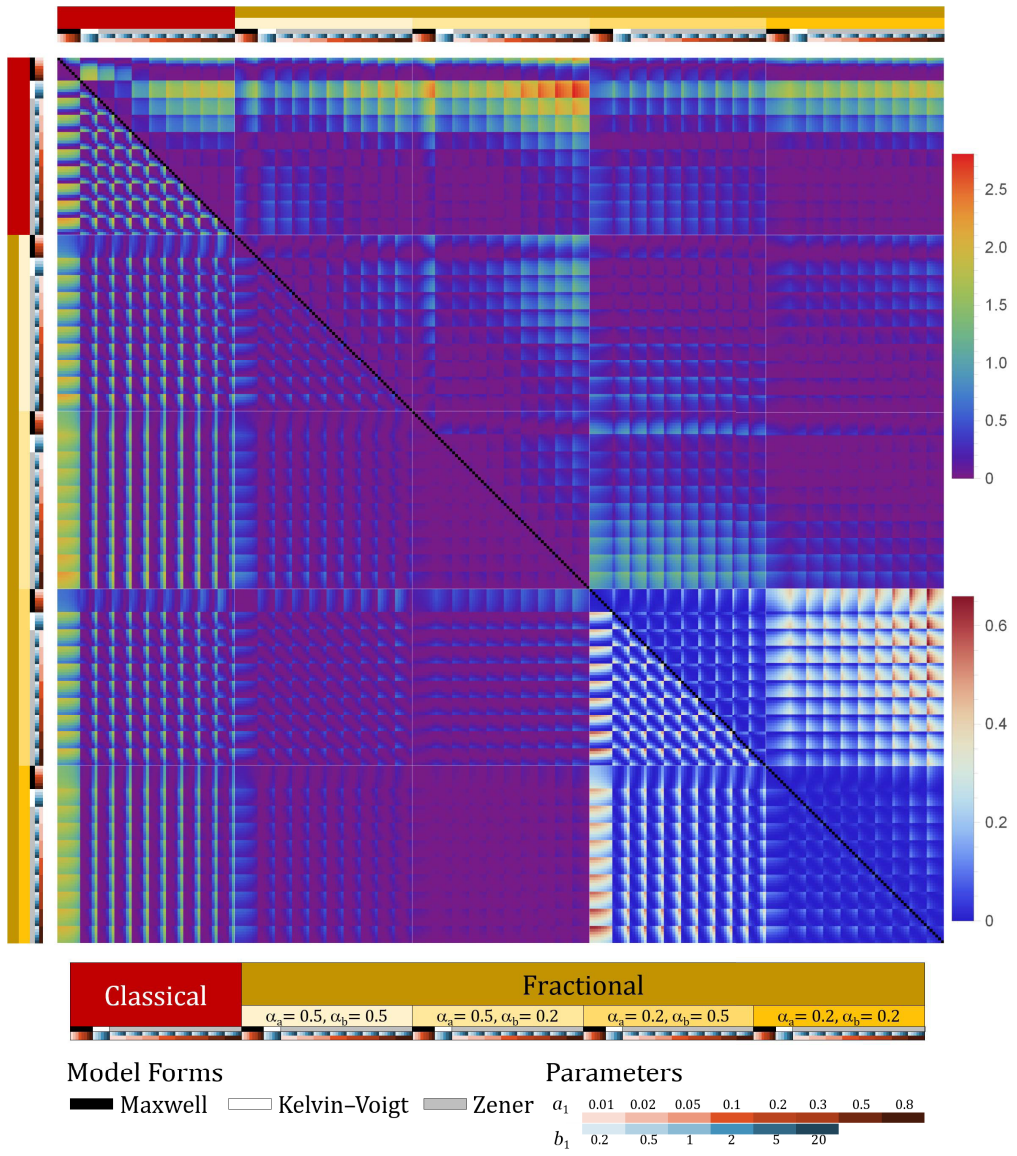

FIG. S7: An illustration using cyclic simple shear with a sine wave form as the example to show how the model responses compare to each other. Each cell shows the similarity score (Eq. 30) between two model forms. The bottom half of the array plot shows the comparison with a frequency of loading of 0.05 Hz and the top half at 5 Hz. The plots for $\alpha_a = 0.2$ uses a different color scale to show more details.

expected (Fig. S14). The Kelvin-Voigt model decays instantaneously after the loading phase and then shows the largest undershoot when the strain is lowered. The Maxwell model shows a linear relaxation but does not have time to decay to 0. As a result, the undershoot during the strain reduction is smaller than at long test duration. The classical Zener model shows a power-law decay that does not have time to reach a plateau and therefore also undershoots more during the strain reduction, compared to the long duration test. The similarity scores pattern between long and short test durations is similar to the one presented in the uniaxial case in the main body of the study (Fig. 6), for slow and fast frequencies, respectively. For the relaxation test, varying the deformation level or nonlinear parameter does not lead to fundamental changes during the decay part. As a result, the similarity score patterns do not change substantially with varying these conditions.

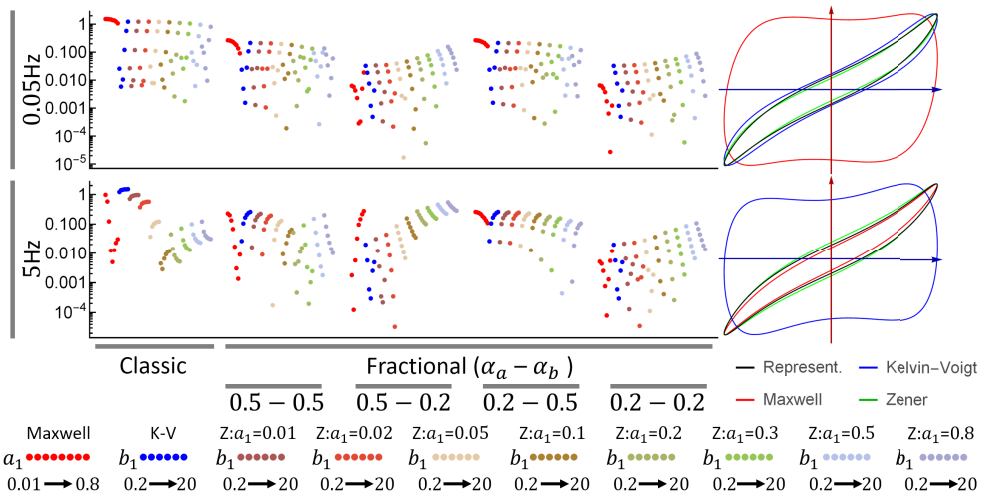

FIG. S8: Examination of each model form in comparison to a representative fractional Zener model exhibiting similar behavior to experimental data. Results at (top) 0.05 and (bottom) 5 Hz are shown. Scatter plots show the similarity scores (Eq. 30) for each model form and parameter combination on the left and the behavior of the *best case* (lowest similarity score) classical Maxwell, Kelvin-Voigt and Zener models on the right.

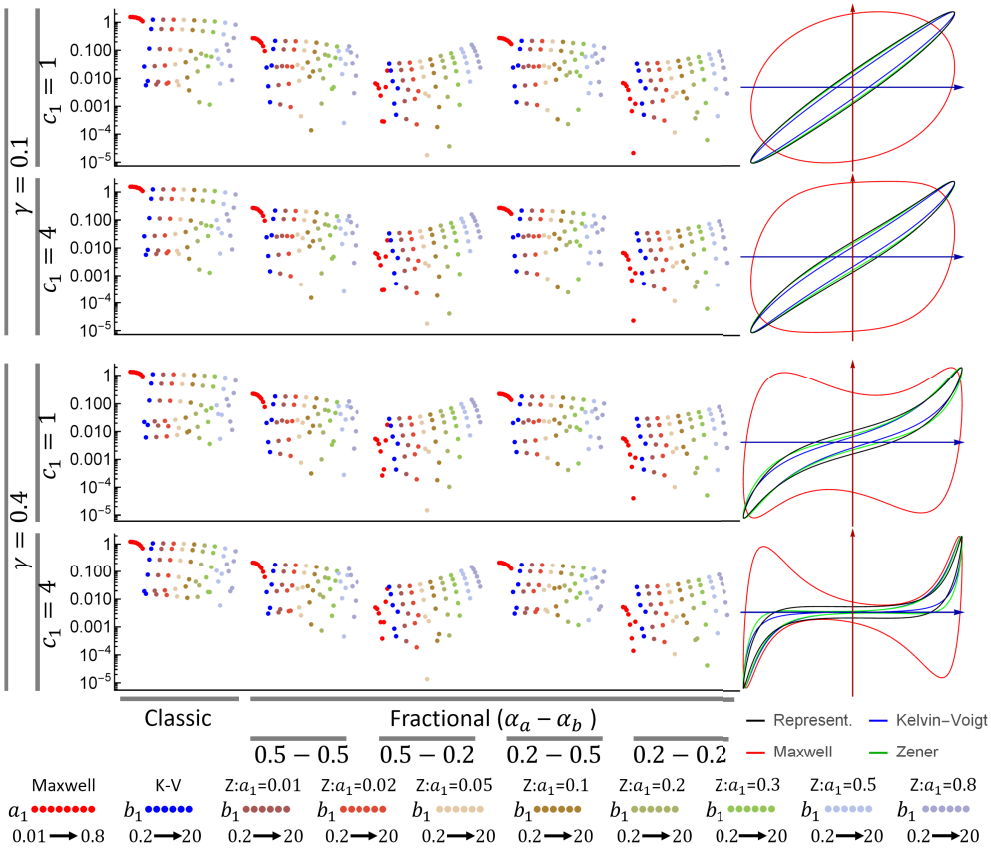

FIG. S9: Results shown the similarity scores at the maximum stretch of 1.1 and 1.4 (row 1&2 and 3&4, respectively) and two different nonlinearity parameters $c_1 = 1$ and $c_1 = 4$ (row 1&3 and 2&4, respectively).

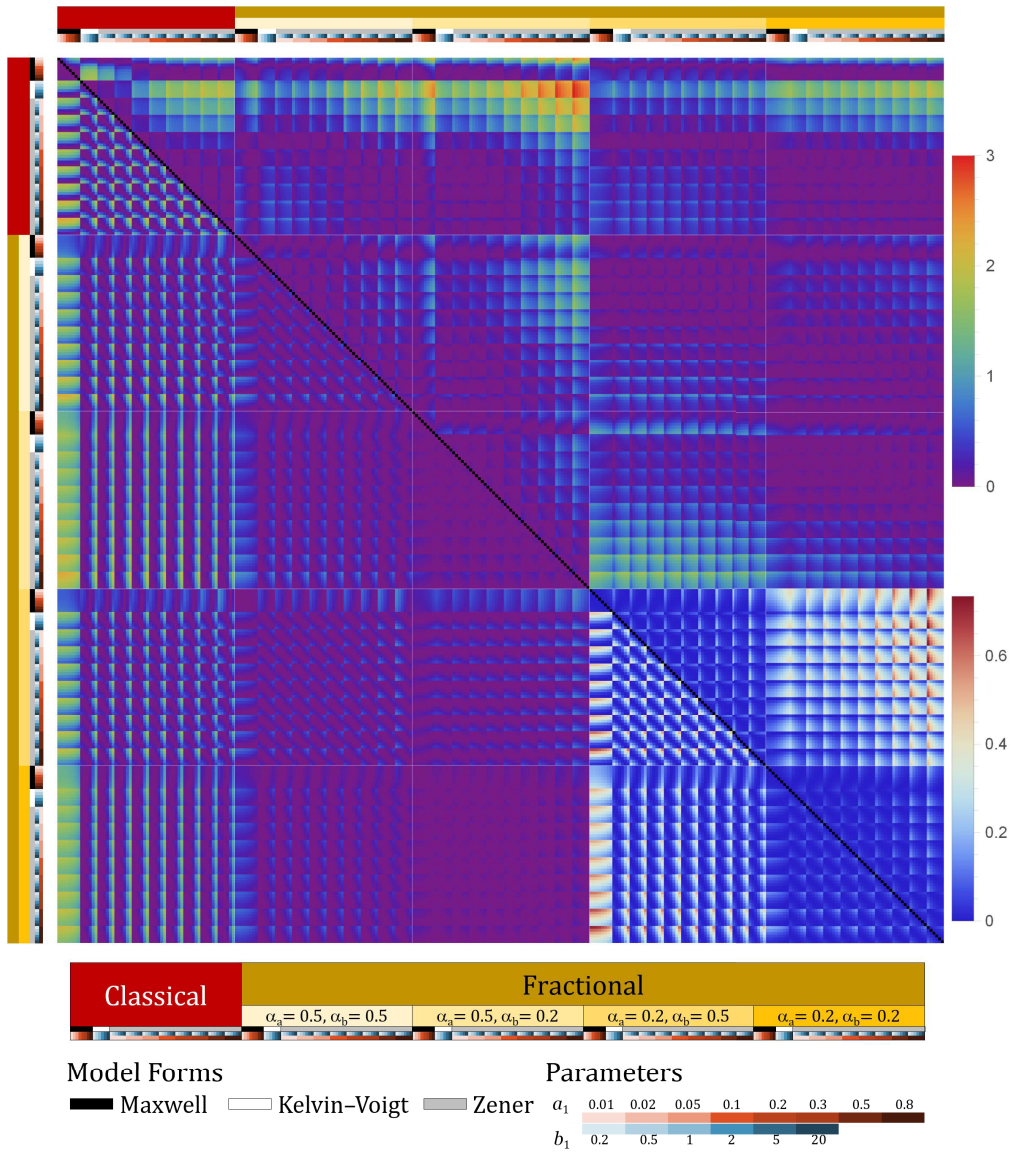

FIG. S10: An illustration using cyclic torsion testing with a sine wave form as the example to show how the model responses compare to each other. Each cell shows the similarity score (Eq. 30) between two model forms. The bottom half of the array plot shows the comparison with a frequency of loading of 0.05 Hz and the top half at 5 Hz. The plots for $\alpha_a = 0.2$ uses a different color scale to show more details.

VII. CREEP TEST CASE

The creep testing result are produced for durations of 0.5 seconds and 50 seconds. Each cycle consists of a loading phase and an unloading phase. The cycle is repeated three time with the last cycle shown below. Similarity scores are shown in Fig. S16, with the last cycle (of 3) shown in Fig. S17. The impact of loading and nonlinear parameters is highlighted in Fig. S18.

For the creep test, the pair-wise comparison of the models across parameter combinations, for short and long test duration, is the most different across tests (Fig. S16). For a long test duration, the classical and fractional Maxwell models are the most dissimilar, as expected. The trend does not appear to be replicated at short test duration, and neither does the classical Kelvin-Voigt model appear to be dissimilar, like in the other tests. Nonetheless, when examining the models' behavior in Fig. S17 for multiple creep-release cycles, the Maxwell model displays strain increase or stagnation, but no recovery, for both tests durations.

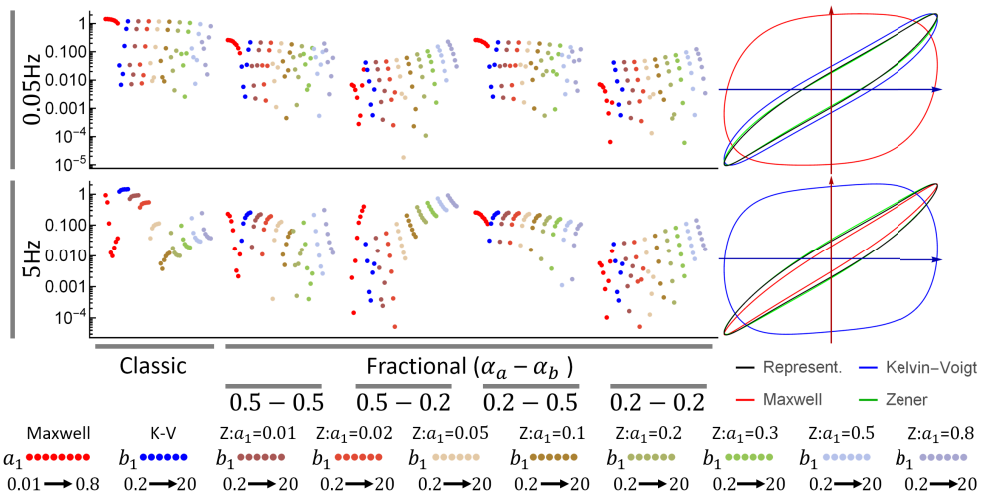

FIG. S11: Examination of each model form in comparison to a representative fractional Zener model exhibiting similar behavior to experimental data. Results at (top) 0.05 and (bottom) 5 Hz are shown. Scatter plots show the similarity scores (Eq. 30) for each model form and parameter combination on the left and the behavior of the *best case* (lowest similarity score) classical Maxwell, Kelvin-Voigt and Zener models on the right.

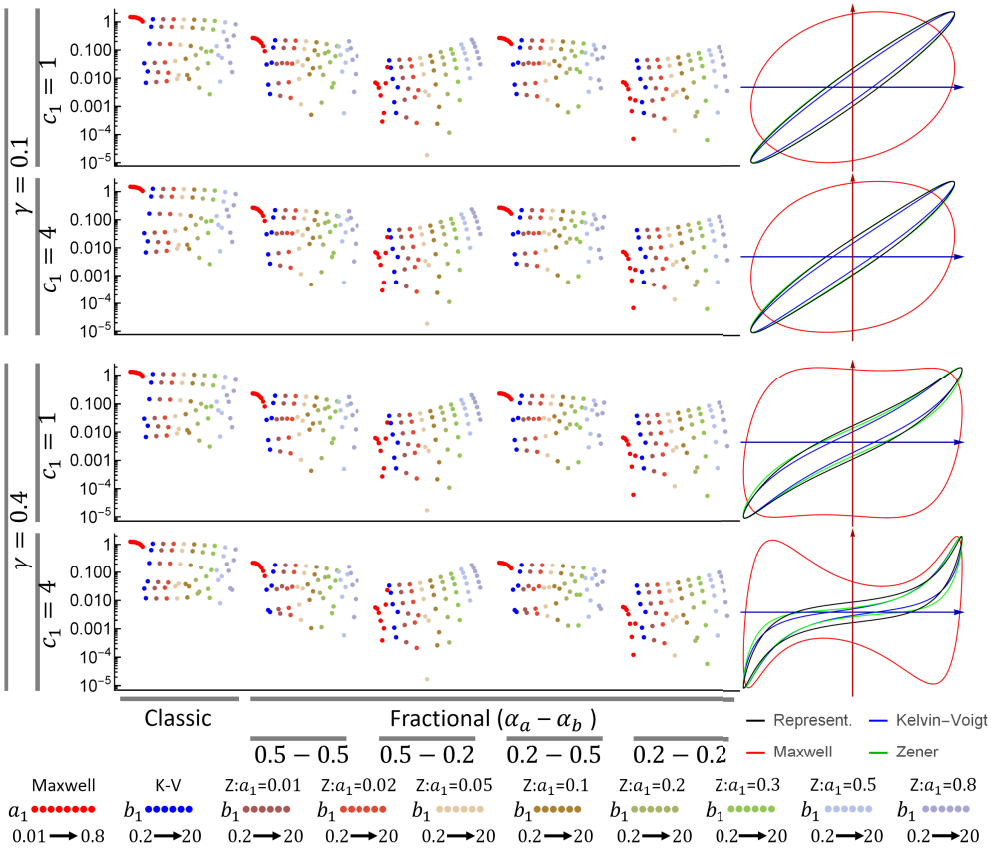

FIG. S12: Results shown the similarity scores at the maximum stretch of 1.1 and 1.4 (row 1&2 and 3&4, respectively) and two different nonlinearity parameters $c_1 = 1$ and $c_1 = 4$ (row 1&3 and 2&4, respectively).

Interestingly, if the test duration is very short, then the classical Kelvin-Voigt model does not have the time to recover and leads to a similar behavior as for the Maxwell model, where the strain keeps increasing

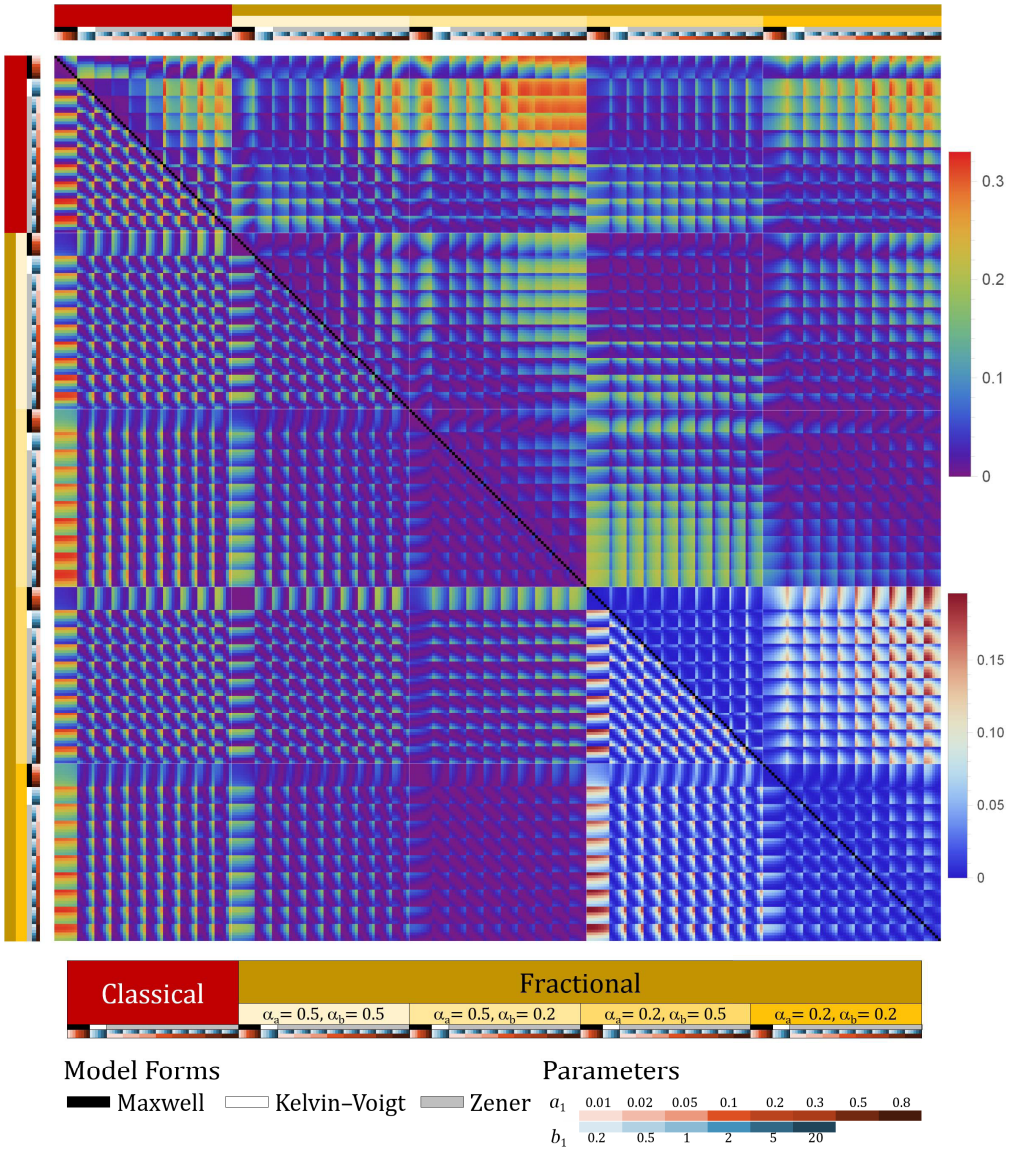

FIG. S13: An illustration using cyclic uniaxial relaxation creep to show how the model responses compare to each other. Each cell shows the similarity score (Eq. 30) between two model forms. The bottom half of the array plot shows the comparison with a cycle period of 50s and the top half at 0.5s. The plots for $\alpha_a = 0.2$ uses a different color scale to show more details.

across multiple cycles. For the classical Zener model, the recovery is faster and the drift of the recovery level increases more clearly for a short test compared to a long test. The fractional Zener model still exhibits a typical tissue creep behavior, with the drift of the recovery level being more obvious in the short duration case. Varying the load applied in the creep test leads to differences in the recovery level (Fig. S18), while variations in the nonlinear parameter c_1 do not lead to any obvious differences in the creep test.

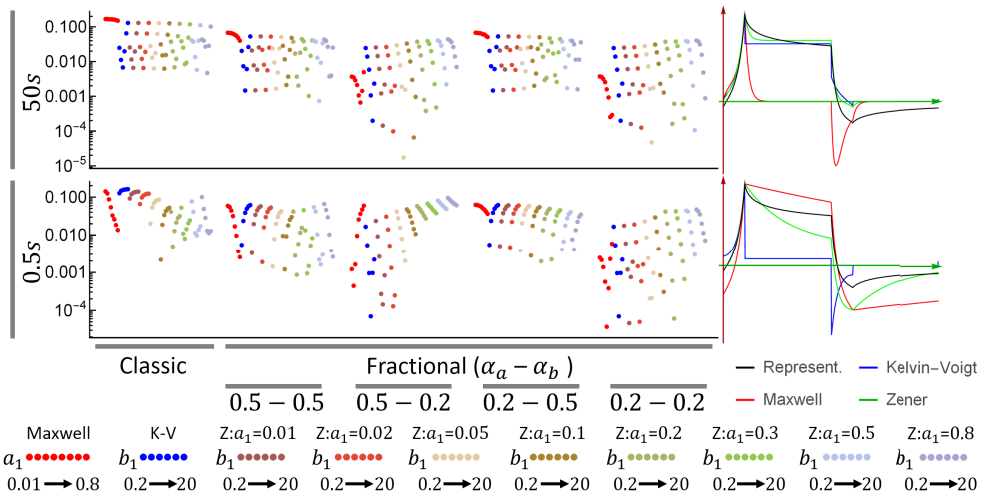

FIG. S14: Examination of each model form in comparison to a representative fractional Zener model exhibiting similar behavior to experimental data. Results at (top) 50s and (bottom) 0.5s are shown. Scatter plots show the similarity scores (Eq. 30) for each model form and parameter combination on the left and the behavior of the *best case* (lowest similarity score) classical Maxwell, Kelvin-Voigt and Zener models on the right.

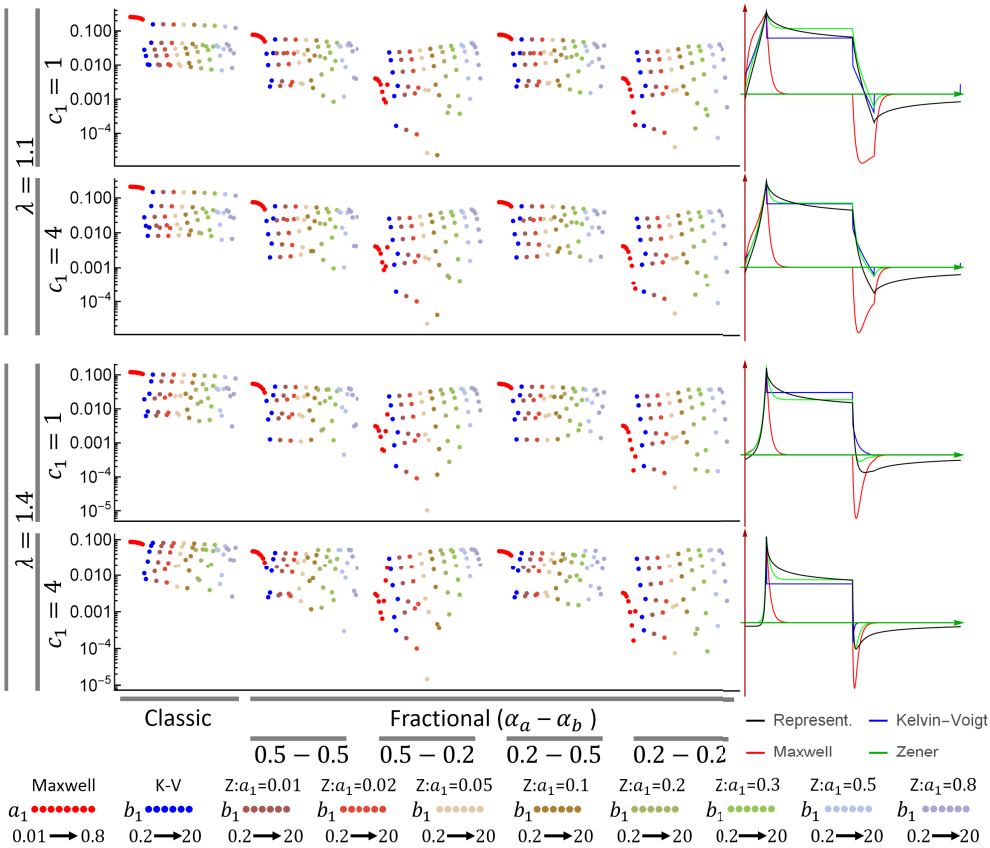

FIG. S15: Results shown the similarity scores at the maximum stretch of 1.1 and 1.4 (row 1&2 and 3&4, respectively) and two different nonlinearity parameters $c_1 = 1$ and $c_1 = 4$ (row 1&3 and 2&4, respectively).

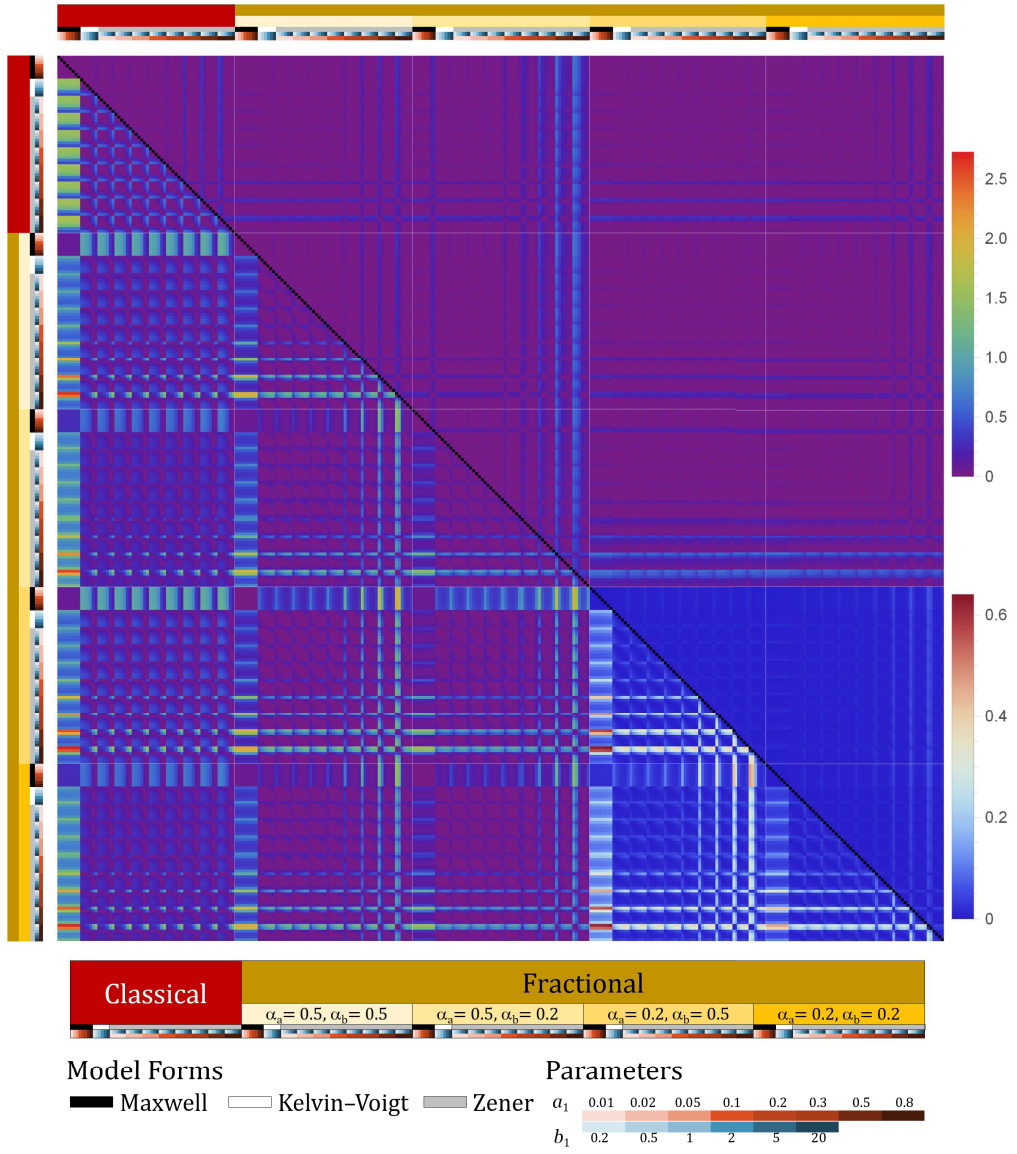

FIG. S16: An illustration using cyclic uniaxial extension creep to show how the model responses compare to each other. Each cell shows the similarity score (Eq. 30) between two model forms. The bottom half of the array plot shows the comparison with a cycle period of 50s and the top half at 0.5s. The plots for $\alpha_a = 0.2$ uses a different color scale to show more details.

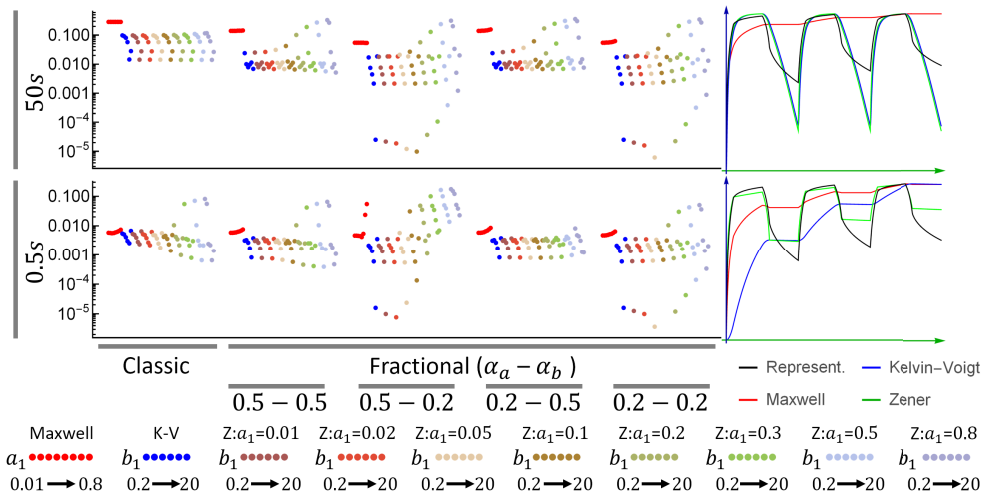

FIG. S17: Examination of each model form in comparison to a representative fractional Zener model exhibiting similar behavior to experimental data. Results at (top) 50s and (bottom) 0.5s are shown. Scatter plots show the similarity scores (Eq. 30) for each model form and parameter combination on the left and the behavior of the *best case* (lowest similarity score) classical Maxwell, Kelvin-Voigt and Zener models on the right. Note the reverse in trend for the Maxwell and Kelvin-Voigt forms and the increase in selectivity for the fractional forms at higher frequency.

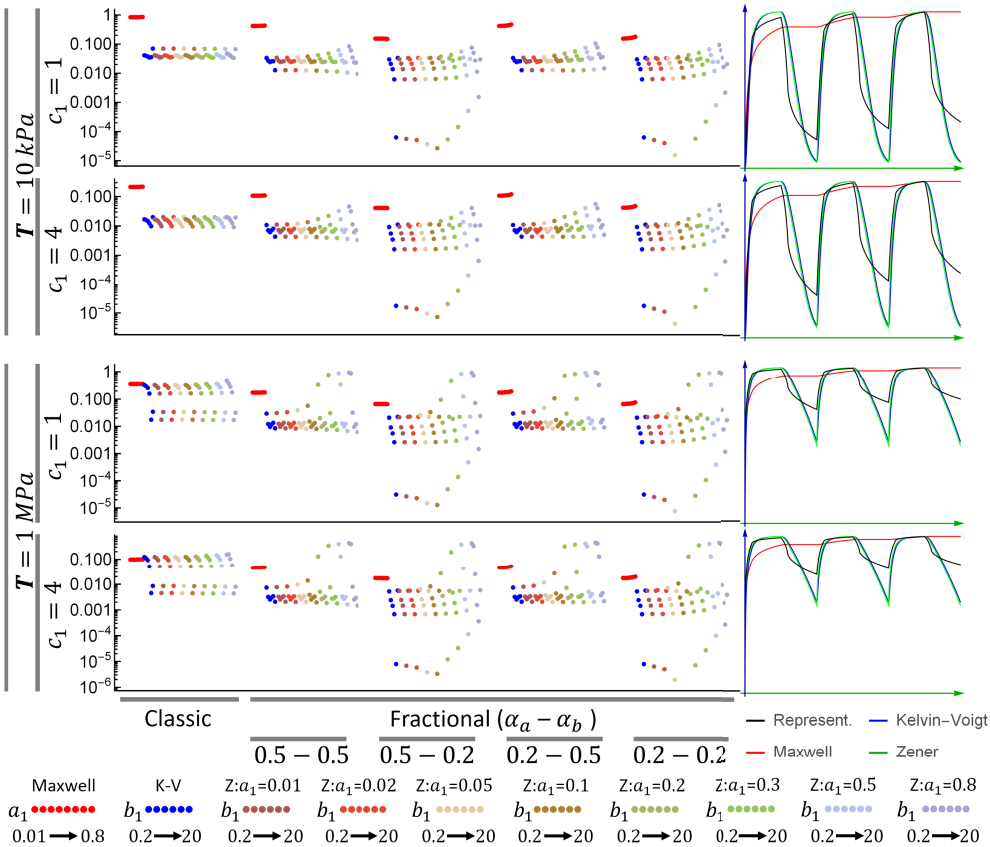

FIG. S18: Results shown the similarity scores at the maximum applied traction of 10 kPa and 1 MPa (row 1&2 and 3&4, respectively) and two different nonlinearity parameters $c_1 = 1$ and $c_1 = 4$ (row 1&3 and 2&4, respectively).